

# Low Temperature Specific Heat of Optimally Doped $\text{BaFe}_{2-x}\text{TM}_x\text{As}_2$ ( $\text{TM} = \text{Co}$ and $\text{Ni}$ ) Single Crystals: Constraint on the Pairing Gap

Bin Zeng, Gang Mu, Bing Shen, Peng Cheng, Huiqian Luo, Huan Yang, Lei Shan, Cong Ren and Hai-Hu Wen<sup>1\*</sup>

<sup>1</sup>*National Laboratory for Superconductivity, Institute of Physics  
and Beijing National Laboratory for Condensed Matter Physics,  
Chinese Academy of Sciences, P.O. Box 603, Beijing 100190, China*

Low temperature specific heat has been measured in optimally doped and highly overdoped non-superconducting  $\text{BaFe}_{2-x}\text{TM}_x\text{As}_2$  ( $\text{TM} = \text{Co}$  and  $\text{Ni}$ ) single crystals. By using the data of the overdoped samples, we successfully removed the phonon contribution of the optimally doped ones, and derived the electronic specific heat coefficient  $\gamma_e$ . Remarkably, we found a continuing temperature dependent  $\gamma_e(T)$  which follows the quadratic relation  $\gamma_e = \gamma_0 + \alpha T^2$  in the low temperature limit. Together with the very small residual term  $\gamma_0$ , linear magnetic field dependence of  $\gamma_e$ , it is concluded that there are either small segments of nodal lines, or point-like nodes in these samples.

PACS numbers: 74.20.Rp, 74.70.Dd, 74.62.Dh, 65.40.Ba

The discovery of superconductivity above 50 K in iron pnictides has added a new member in the family of unconventional high temperature superconductors.[1] One of the key issues here is about the superconducting pairing mechanism. Theoretically it was suggested that the pairing may be established via inter-pocket scattering of electrons between the hole pockets (around  $\Gamma$  point) and electron pockets (around M point), leading to the so-called  $S^\pm$  pairing manner.[2–5] Experimental results about the pairing symmetry remain highly controversial leaving the perspectives ranging from  $S^{++}$ -wave, to  $S^\pm$  and to d-wave.[6–15] Although evidence for a nodal gap has been accumulated in  $\text{LaFePO}$ [6, 7] and  $\text{Ba}(\text{FeAs}_{1-x}\text{P}_x)_2$  systems[13], in the charge doped 122, the experimental data point to the existence of isotropic gaps, especially in the optimally doped samples.[8, 11, 12] The penetration depth measurements indicate a quadratic temperature dependence  $\Delta\lambda \propto 1 - (T/T_c)^2$  when the measuring inductive current is flowing along FeAs-plane.[12] And it becomes more linear like when the detecting current has a c-axis component, indicating the possibility of nodes along c-axis but nodeless along FeAs-plane.[16] This is further strengthened by the recent thermal conductivity measurements which suggest the possible existence of a horizontal nodal line.[17] In this Letter, we present the data of low temperature specific heat (SH) in  $\text{BaFe}_{2-x}\text{TM}_x\text{As}_2$  ( $\text{TM} = \text{Co}$  and  $\text{Ni}$ ) single crystals. A unique quadratic temperature dependence  $\gamma_e = \gamma_0 + \alpha T^2$  was found in the low-T limit. This is different from the expectation for a d-wave superconductor in the clean limit  $C_e \propto T^2$ . Combining with the very small  $\gamma_0$  and the linear field dependence of  $\gamma_e$ , it is tempting to conclude the existence of small segments of nodal lines or point-like nodes, being consistent with the recent five band tight binding calculations.[18]

The Co- and Ni-doped  $\text{BaFe}_2\text{As}_2$  single crystals were grown by the self-flux method[19, 20]. In order to get the phonon contribution of SH, we also measured an overdoped non-superconducting sample as the reference for

each kind of dopant. The typical dimension of the single crystals for specific heat measurements was  $3 \times 3 \times 0.4 \text{ mm}^3$ . The SH measurements were done with the thermal relaxation method on the Quantum Design instrument physical property measurement system (PPMS) with the temperature down to 1.8 K and magnetic field up to 9 T. To improve the resolution, the field dependence of the sensor on the measuring chip was calibrated in advance.

In Fig.1(a), we show the temperature dependence of resistivity for four samples:  $\text{BaFe}_{2-x}\text{Co}_x\text{As}_2$  with  $x = 0.16$  and  $0.60$ , and  $\text{BaFe}_{2-x}\text{Ni}_x\text{As}_2$  with  $x = 0.10$  and  $0.30$ , respectively. The onset transition temperatures determined at  $\rho = 95\%\rho_n$  for  $\text{BaFe}_{1.84}\text{Co}_{0.16}\text{As}_2$  and  $\text{BaFe}_{1.9}\text{Ni}_{0.1}\text{As}_2$  are 24.2 K and 20.5 K, respectively, which are close to the optimal doping points. The sharp transitions near  $T_c$  in the dc magnetization and resistivity measurements indicate the good quality of the samples. No superconductivity was detected in  $\text{BaFe}_{1.4}\text{Co}_{0.6}\text{As}_2$  and  $\text{BaFe}_{1.7}\text{Ni}_{0.3}\text{As}_2$  down to 1.8 K.

In Fig.2, we present the SH of the superconducting and non-superconducting samples under zero field for each dopant. Sharp and clear SH anomalies near  $T_c$  for the samples  $\text{BaFe}_{1.84}\text{Co}_{0.16}\text{As}_2$  and  $\text{BaFe}_{1.9}\text{Ni}_{0.1}\text{As}_2$  can be seen. For all samples investigated here, the Schottky anomalies are negligible. For each dopant, one can see that the SH in the normal state for the superconducting and non-superconducting samples share a very similar temperature dependence. This allows us to use the phonon part of SH of the non-superconducting sample as the reference, and subtract it safely for the superconducting one.

In order to extract the electronic SH of the superconducting samples, people usually apply a magnetic field to destroy the superconductivity, and measure the SH of the normal state. For the iron-based superconductors, however, the upper critical field is too high to be reached.[21] So we employ the method suggested in the literatures[22, 23]. Here we take the overdoped non-superconducting sample as the references. Suppose that

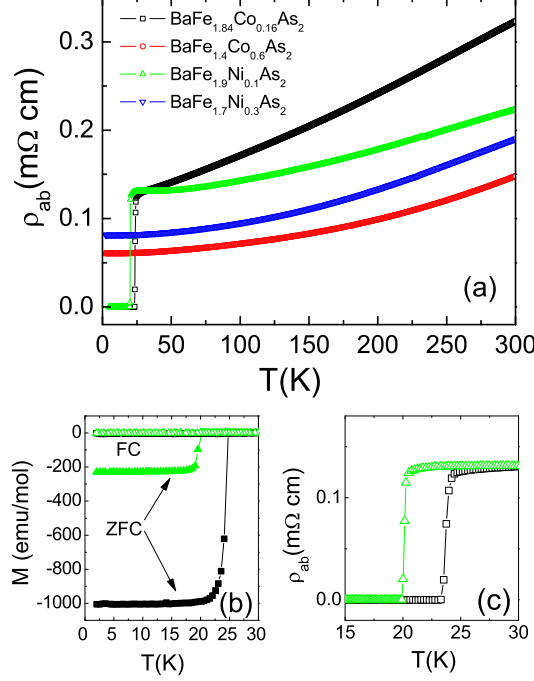


FIG. 1: (color online) (a) Temperature dependence of resistivity of the optimally doped and highly overdoped non-superconducting  $\text{BaFe}_{2-x}\text{TM}_x\text{As}_2$  ( $\text{TM} = \text{Co}$  and  $\text{Ni}$ ) single crystals at zero field. (b) Temperature dependence of dc magnetization for the two superconducting samples. The enlarged view of resistivity for the two superconducting samples is shown in (c).

the phonon contributions of the non-superconducting sample is  $C_{ph}^N(T)$ , which can be obtained by subtracting the linear electronic term from the total SH, and that of the superconducting sample is  $C_{ph}^S(T)$ , we naturally have  $C_{ph}^S(T) = a \cdot C_{ph}^N(b \cdot T)$ . Here  $a$  and  $b$  are fitting parameters which should be close to unity. Using a least-squares fit of our data above  $T_c$ , we determined  $a$  and  $b$  to be 1.000, 1.013 for the Co-doped sample, and 0.98, 0.99 for the Ni-doped one, indicating that the phonon contributions of the superconducting sample and the overdoped non-superconducting one are indeed very close to each other. Although the antiferromagnetic (AF) spin fluctuation is very strong in the optimally doped sample and negligible in the overdoped one[24], the SH concerns mainly the  $Q = 0$  scattering and is sensitive only to the quasiparticle density of states (DOS) at  $E_F$ . The entropy conservation (not shown here) obtained by this treatment supports above argument. The electronic SH of the superconducting sample can then be obtained through

$$C_e^S(T) = C_{tot}^S(T) - C_{ph}^S(T) = C_{tot}^S(T) - a \cdot C_{ph}^N(b \cdot T), \quad (1)$$

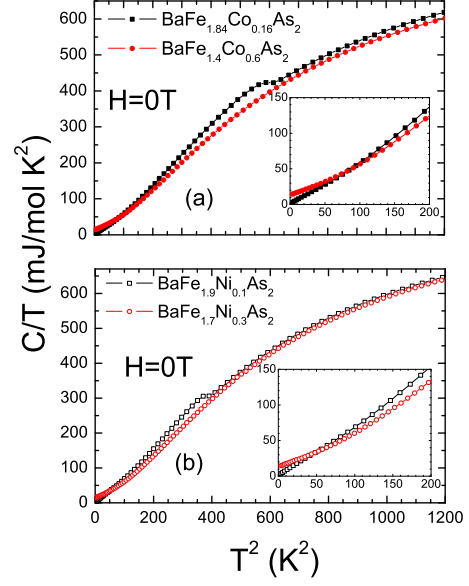


FIG. 2: (color online) Raw data of the temperature dependence of specific heat for the  $\text{BaFe}_{2-x}\text{TM}_x\text{As}_2$  ( $\text{TM} = \text{Co}$  and  $\text{Ni}$ ) single crystals. The enlarged views of the same data are presented as insets in (a) and (b), respectively.

where  $C_{tot}^S(T)$ ,  $C_e^S(T)$  are the total and the electronic SH of the superconducting sample, respectively.

The obtained electronic SH for Co- and Ni-doped samples are shown in Fig.3. Surprisingly, we found a continuing temperature dependent electronic SH coefficient  $\gamma_e(T)$ , which follows the quadratic relation  $\gamma_e = \gamma_0 + \alpha T^2$  in the low-T limit (see the insets of Fig.3). The parameters of  $\gamma_0$  were determined from the fitting: 1.53 mJ/mol  $\text{K}^2$  and 1.49 mJ/mol  $\text{K}^2$ , for the superconducting Co- and Ni-doped samples, respectively, which are rather small compared to the values reported in literatures, indicating the cleanness of our samples. In order to get a comprehensive understanding, we used the BCS formula to fit our data

$$\gamma'_e = \frac{4N_F}{k_B T^3} \int_0^{+\infty} \int_0^{2\pi} \frac{e^{\zeta/k_B T}}{(1 + e^{\zeta/k_B T})^2} (\varepsilon^2 + \Delta^2(\theta, T) - \frac{T}{2} \frac{d\Delta^2(\theta, T)}{dT}) d\theta d\varepsilon, \quad (2)$$

where  $\gamma'_e = \gamma_e - \gamma_0$ ,  $\zeta = \sqrt{\varepsilon^2 + \Delta^2(T, \theta)}$ ,  $N_F$  the DOS at the Fermi energy. We use four different gap structures to fit the data: single isotropic s-wave gap ( $S_{iso}$ ), single anisotropic gap with a d-wave feature ( $S_d$ :  $\Delta = \Delta_0 |\cos 2\theta|$ ), mixture of two:  $S_{iso} + S_d$  and two isotropic gaps  $S_{iso1} + S_{iso2}$ . In the latter two cases, the  $\gamma_e$  was calculated through a linear combination of the two

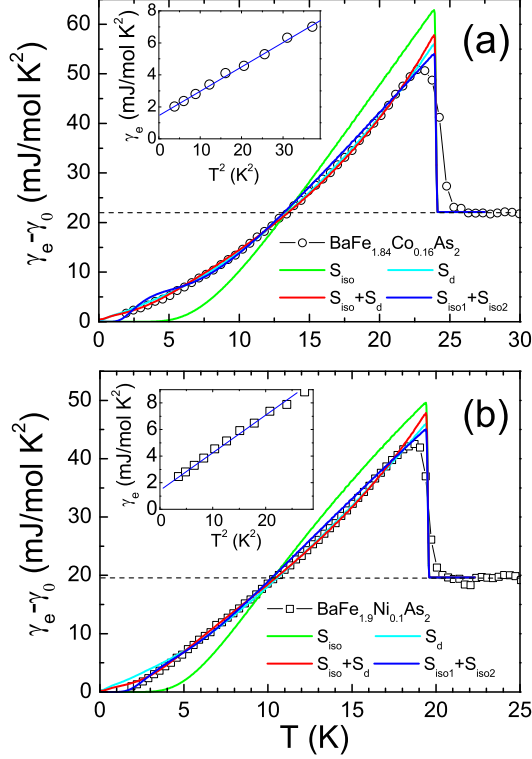


FIG. 3: (color online) The electronic specific heat of the optimally doped superconducting samples (a)  $\text{BaFe}_{1.84}\text{Co}_{0.16}\text{As}_2$  and (b)  $\text{BaFe}_{1.9}\text{Ni}_{0.1}\text{As}_2$ . These data were obtained by removing the phonon contribution (see text). The insets show the enlarged view of the low temperature specific heat, a quadratic temperature dependence  $\gamma_e = \gamma_0 + \alpha T^2$  can be clearly seen. Four different models: single isotropic s-wave gap ( $S_{iso}$ ), single anisotropic gap with a d-wave feature ( $S_d$ ), mixture of two:  $S_{iso} + S_d$  and  $S_{iso1} + S_{iso2}$  were used to fit the data.

components. The fitting curves are shown by the colored lines in Fig.3, and the fitting parameters are listed in Table I and Table II, respectively. One can see that the single isotropic s-wave model can not fit the data at all, while the fittings with  $S_d$ ,  $S_{iso} + S_d$  and  $S_{iso1} + S_{iso2}$  can roughly describe the data. However, if we explore the data in more detail, we can see that the fit of  $S_{iso1} + S_{iso2}$  model has an overall deviation to the data, and single  $S_d$  can roughly fit the data except in low-T region, where the fitting result is higher than the experimental data. The  $S_{iso} + S_d$  model seems to give the best fitting in the whole temperature region. The multigap scenario ( $S_{iso} + S_d$ ) with a very small s-wave gap of about 2 meV, which accounts for less than 30% of the total quasiparticle DOS, seems possible. The global fitting with  $S_{iso} + S_d$ , together with the relationship  $\gamma_e = \gamma_0 + \alpha T^2$  in the low-T limit, suggest that anisotropic gaps, possibly with nodes, may

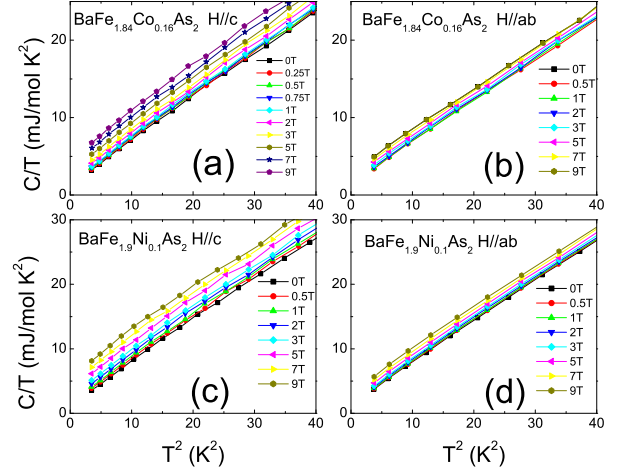


FIG. 4: (color online) Temperature dependence of the specific heat  $C/T$  in the low temperature region for  $\text{BaFe}_{1.84}\text{Co}_{0.16}\text{As}_2$  and  $\text{BaFe}_{1.9}\text{Ni}_{0.1}\text{As}_2$  with the magnetic field aligned with FeAs-plane and c-axis.

TABLE I: Fitting parameters with different models for the Co-doped sample.

model	$\Delta_1(\text{meV})$	fraction-1	$\Delta_2(\text{meV})$	fraction-2
$S_{iso}$	4.2	100%	-	-
$S_d$	5.4	100%	-	-
$S_{iso} + S_d$	2.4	17%	5.9	83%
$S_{iso1} + S_{iso2}$	1.0	25%	4.25	75%

TABLE II: Fitting parameters with different models for the Ni-doped sample.

model	$\Delta_1(\text{meV})$	fraction-1	$\Delta_2(\text{meV})$	fraction-2
$S_{iso}$	3.1	100%	-	-
$S_d$	4.1	100%	-	-
$S_{iso} + S_d$	2.0	29%	4.7	71%
$S_{iso1} + S_{iso2}$	1.15	29%	3.3	71%

exist in these FeAs-based superconductors.

To explore whether the quadratic temperature dependence  $\gamma_e = \gamma_0 + \alpha T^2$  is due to the presence of line nodes, we measured also the magnetic field dependence of  $\gamma_e$ . The data are plotted as  $C/T$  vs.  $T^2$  in Fig.4. One can see the roughly linear behavior in the low-T region. It is clear that the field induced enhancement of the electronic SH is larger when the field is along c-axis than along FeAs-plane, indicating that the upper critical field is higher along FeAs-plane than along c-axis.[25] By doing a linear extrapolation of the data in Fig.4 to zero K, we get the field dependence of the electron SH coefficient  $\gamma_e(H)$ , as shown in the upper part of Fig.5. It is clear that  $\gamma_e(H)$  increase linearly with magnetic field for the two samples in both alignments. This excludes both the vertical (like a d-wave) or horizontal line nodes (bottom-left picture in

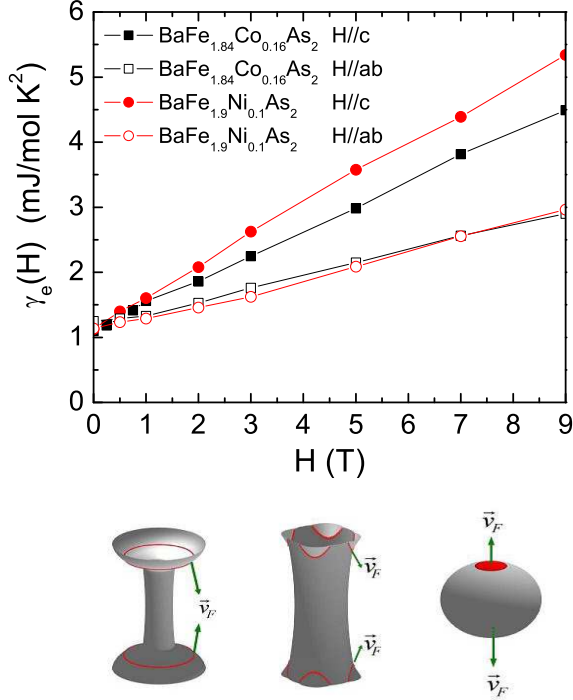


FIG. 5: (color online) Magnetic field dependence of the electronic specific heat for the samples  $\text{BaFe}_{1.84}\text{Co}_{0.16}\text{As}_2$  and  $\text{BaFe}_{1.9}\text{Ni}_{0.1}\text{As}_2$  when the field is aligned along FeAs-plane and c-axis. A rough linear feature was observed in all four cases. The bottom part illustrates the possible gap nodes on the  $\Gamma$  Fermi surfaces: (left) horizontal nodal lines; (middle) small segments of nodal lines (shown by the red lines); (right) point nodes on the 3D Fermi pockets.

Fig.5), since otherwise, as found in cuprate superconductors, a square root relation  $\gamma_e(H) \propto \sqrt{H}$ [26] in the clean limit, or a curved feature  $\gamma_e(H) \propto H/H_{c2} \log(BH_{c2}/H)$  with impurity scattering[27] should be observed.

Although the quadratic temperature dependence  $\gamma_e = \gamma_0 + \alpha T^2$  can also be attributed to the DOS induced by the impurity scattering within the  $S^\pm$  model[28–30], we would argue that this is unlikely for the following reasons. Firstly, the exponent “2” here may be achieved in the case of strong pair breaking[30], which is in contrast to the small value of  $\gamma_0 \sim 1.5 \text{ mJ/mol K}^2$  ( $\leq 7.5\% \gamma_n$ ). Furthermore, according to Onari et al.,[29], even with such a small amount impurities (assuming to induce the large momentum scattering), the superconductivity may not survive within the  $S^\pm$  model. Secondly, it is not straightforward to understand the linear field dependence of  $\gamma_e(H) - \gamma_0 \propto H$  with this picture. In order to reconcile the observations of a small  $\gamma_0$ ,  $\gamma_e = \gamma_0 + \alpha T^2$  and  $\gamma_e(H) - \gamma_0 \propto H$ , we propose that nodes, in the form of point-like or small segments, may exist in our present samples. As indicated by the five-band tight-

binding calculations,[18] small segments of nodal lines (or called as accidental nodes) may exist on the hole-pockets near  $k_z = \pm\pi$ , which is depicted by the middle-bottom cartoon picture of Fig.5. An alternative interpretation would assume the extreme case of point-like nodes with a closed 3D Fermi pocket. It is natural that the pairing interaction by mediating the AF spin fluctuations should be very weak on the right top or bottom of these 3D pockets where the Fermi velocity is along c-axis (see the bottom-right picture of Fig.5), therefore the gap amplitude becomes negligible. Actually these two pictures can reconcile all the observations in this work. In a system with point nodes (or small segments of line nodes), it is anticipated that  $N_F \propto E^2$ , since the Doppler shift energy of  $E_H \propto \sqrt{H}$ , we have  $N_F \propto H$ . Meanwhile, the relation  $\gamma_e = \gamma_0 + \alpha T^2$  is also anticipated by the point-like nodes.

In summary, the electronic specific heat on the optimally Ni- and Co-doped superconducting samples was derived by successfully removing the phonon contributions. A quadratic temperature dependence of  $\gamma_e = \gamma_0 + \alpha T^2$  in the low-T limit was discovered. The global temperature dependence of  $\gamma_e$  can be fitted with a two-component model with possible nodes. However the linear field dependence  $\gamma_e(H) \propto H$  observed with the magnetic field along FeAs-plane and c-axis excludes the existence of either vertical or horizontal line nodes. The results put strong constraint on the pairing gap and can be reconciled by the model of small segments of line nodes or point-like nodes.

We appreciate the discussions with P. Hirschfeld, S. Graser, A. Chubukov, Y. Matsuda, G. Stewart, G. Q. Zheng and Z. Tes̃anović. This work is supported by the NSF of China, the Ministry of Science and Technology of China (973 projects: 2006CB601000, 2006CB921107, 2006CB921802), and Chinese Academy of Sciences within the knowledge innovation program.

\* hhwen@aphy.iphy.ac.cn

- 
- [1] Y. Kamihara *et al.*, J. Am. Chem. Soc. **130**, 3296 (2008).
  - [2] I. I. Mazin *et al.*, Phys. Rev. Lett. **101**, 057003 (2008).
  - [3] K. Kuroki *et al.*, Phys. Rev. Lett. **101**, 087004 (2008).
  - [4] F. Wang *et al.*, Phys. Rev. Lett. **102**, 047005 (2009).
  - [5] Z. J. Yao, J. X. Li, Z. D. Wang, New J. Phys. **11**, 025009 (2009).
  - [6] J. D. Fletcher *et al.*, Phys. Rev. Lett. **102**, 147001 (2009).
  - [7] C. W. Hicks *et al.*, Phys. Rev. Lett. **103**, 127003 (2009).
  - [8] H. Ding *et al.*, Europhys. Lett. **83**, 47001 (2008).
  - [9] K. Hashimoto *et al.*, Phys. Rev. Lett. **102**, 017002 (2009).
  - [10] H.-J. Grafe *et al.*, Phys. Rev. Lett. **101**, 047003 (2009).
  - [11] X. G. Luo *et al.*, Phys. Rev. B **80**, 140503(R) (2009).
  - [12] R. T. Gordon *et al.*, Phys. Rev. Lett. **102**, 127004 (2009).
  - [13] C. Martin *et al.*, Phys. Rev. B **80**, 020501(R)(2009).
  - [14] K. Hashimoto *et al.*, arXiv:0907.4399 (2010). Y. Nakai *et al.*, Phys. Rev. B **81**, 020503(R)(2010).
  - [15] T. Sato *et al.*, J. Phys. Soc. Jpn. **77**, 063708 (2008).

- [15] G. Mu *et al.*, Chin. Phys. Lett. **25**, 2221 (2008). G. Mu *et al.*, Phys. Rev. B **79**, 174501 (2009).
- [16] C. Martin *et al.*, Phys. Rev. B **81**, 060505(R)(2010).
- [17] J. Ph. Reid *et al.* arXiv:1004.3804.
- [18] S. Graser, T. A. Maier, P. J. Hirschfeld, D. J. Scalapino, New J. Phys. **11**, 025016 (2009).
- [19] L. Fang *et al.*, Phys. Rev. B **80**, 140508(R) (2009).
- [20] M. Y. Wang *et al.*, arxiv: 1002.3133 (2010).
- [21] J. S. Kim *et al.*, Phys. Rev. B **81**, 214507 (2010).
- [22] P. Popovich *et al.*, arXiv:1001.1074 (2010).
- [23] K. Gofryk *et al.*, Phys. Rev. B **81**, 184518(2010).
- [24] F. L. Ning *et al.*, Phys. Rev. Lett. **104**, 037001 (2010).
- [25] Z. S. Wang *et al.*, Phys. Rev. B **78**, 140501(R) (2008).
- [26] G. E. Volovik *et al.*, JETP Lett. **58**, 469 (1993).
- [27] C. Kübert and P. J. Hirschfeld, Solid State Commun. **105**, 459 (1998).
- [28] Y. Bang *et al.*, Phys. Rev. B **79**, 054529 (2009).
- [29] S. Onari and H. Kontani, Phys. Rev. Lett. **103**, 177001 (2009)
- [30] R. T. Gordon *et al.*, Phys. Rev. B **81**, 180501(R) (2010).